Average charge states of heavy and superheavy ions passing through a rarified gas: Theory and experiment

J. Khuyagbaatar,[1,*] V. P. Shevelko,[2] A. Borschevsky,[1] Ch. E. Düllmann,[1,3,4] I. Yu. Tolstikhina,[2,5] and A. Yakushev[3]

[1]*Helmholtz-Institut Mainz, 55099 Mainz, Germany*

[2]*Levedev Physical Insitute, Leninskii Prospect 53, 119991 Moscow, Russia*

[3]*GSI Helmholtzzentrum für Schwerionenforschung GmbH, 64291 Darmstadt, Germany*

[4]*Johannes Gutenberg-Universität Mainz, 55099 Mainz, Germany*

[5]*Moscow Institute of Physics and Technology, 141700 Dolgoprudny, Russia*

(Received 29 July 2013; published 8 October 2013)

The average charge states $\bar{q}$ of heavy and superheavy ions (atomic numbers $Z = 80$–114) passing through He gas are studied experimentally and theoretically. Experimental data were measured at the gas-filled recoil separator, i.e., the TransActinide Separator and Chemistry Apparatus (TASCA) at GSI Darmstadt, for ion energies of a few hundred keV/u at gas pressures of 0.2 to 2.0 mbar. An attempt is made to describe experimental $\bar{q}$ values by means of atomic calculations of the binding energies and electron-loss and electron-capture cross sections. The influence of the gas-density effect is included in the calculations. The calculated $\bar{q}$ reproduce the experimental values for elements with $Z = 80$–114 within 20%. A comparison with different semiempirical models is presented as well, including a local fit of high accuracy, which is often used in superheavy-element experiments to estimate the average charge states of heavy ions, e.g., at the gas-filled recoil separator TASCA. The $\bar{q}$ values for elements with $Z = 115$, 117, 119, and 120 at He-gas pressure of 0.8 mbar are predicted.

DOI: 10.1103/PhysRevA.88.042703 PACS number(s): 34.50.Fa, 31.15.A−, 25.70.Gh

I. INTRODUCTION

The behavior of the charge-state distribution of heavy ions passing through a gas-filled volume is an important topic of heavy-ion beam physics. The charge states of these ions fluctuate in the gaseous volume due to the competing charge-changing processes—electron capture (EC) and electron loss (EL) [1]. After a number of subsequent charge-changing collisions, the charge-state distribution becomes dynamically stable and reaches its equilibrium with an average charge state $\bar{q}$.

In the past, many fundamental aspects of charge-changing collisions were established, both experimentally and theoretically, by studying the EC and EL cross sections of stable heavy ions with atomic numbers up to $Z = 92$ in rarefied gases [1].

Presently, elements with atomic numbers up to $Z = 118$ are becoming experimentally accessible due to intensive research on the synthesis of superheavy nuclei in nuclear fusion-evaporation reactions [2–4]. Different in-flight separation methods are used to isolate these superheavy ions from the products of other nuclear reactions. One of the most powerful separation techniques is based on the charge-state equilibrium phenomena. Gas-filled separators employing this technique are widely used [5–9].

The synthesis of superheavy elements with atomic numbers $Z = 113$–118 in ^{48}Ca-induced reactions with various actinide targets was carried out at the Dubna Gas-Filled Recoil Separator (DGFRS), which was filled with dilute hydrogen molecular gas [4]. Some of these results were confirmed by independent studies at other, He-gas-filled separators such as the Berkeley Gas-filled Separator (BGS) at LBNL Berkeley [10,11], and the TransActinide Separator and Chemistry Apparatus (TASCA) at GSI Darmstadt [12,13]. The available experimental data support the Z assignments of the superheavy elements, and those with $Z = 114$ and 116 [14] were recently officially named flerovium (Fl) and livermorium (Lv), respectively [15]. Such experimental research on superheavy elements provides new information on their average charge states in dilute gases, thus making a great impact on atomic physics.

Semiempirical and semiclassical formulas are often used for the estimation of the $\bar{q}$ of heavy ions in a gas (see, e.g., [1]). However, in practice, the results of these formulas often fail to describe the experimental data with the needed accuracy. This is related to the complexities of the theoretical description of the charge-changing processes, which depend on the atomic numbers of the heavy ion and the gas atoms, velocity and the atomic shell structure of the ion, and the gas density.

In this paper, we present experimental data on the $\bar{q}$ of heavy ions with atomic numbers $Z = 80$–114 in the energy range of a few hundred keV/u measured in He gas at pressures around 0.8 mbar. The experimental data are compared to the predictions of several semiempirical formulas.

Alongside these experimental data and the semiempirical approaches, we present an attempt to describe the $\bar{q}$ of the heavy and superheavy ions and their dependence on the gas pressure within the framework of atomic physics. Our theoretical description of the $\bar{q}$ is based on the calculations of the binding energies, the wave functions, and the cross sections of charge-changing processes. The present calculations of $\bar{q}$ values allowed us to describe our experimental data and those measured earlier at TASCA with 20% accuracy. The dependence of the experimental $\bar{q}$ on the He-gas pressure is also discussed within the present theoretical treatment.

Furthermore, the $\bar{q}$ values are theoretically and semiempirically predicted for elements with $Z = 115$, 117, 119, and 120, which were the focus of the recent experiments at TASCA [16–18].

*J.Khuyagbaatar@gsi.de

II. EXPERIMENTAL AVERAGE CHARGE STATES OBTAINED AT TASCA

Heavy ions considered in this work were produced as evaporation residues (ERs) of excited compound nuclei formed in nuclear fusion reactions between the accelerated ions of stable elements (beam) and the heavy atoms of solid targets at the gas-filled separator TASCA. The beams were accelerated by the Universal Linear Accelerator (UNILAC) up to energies around the Coulomb barrier. Solid targets with typical thicknesses of 0.3–0.6 mg/cm^2 were used. The magnetic system of TASCA consists of a deflecting dipole and a focusing quadrupole doublet and was operating in the ion-optical "high transmission mode" [9].

Evaporation residues leaving the target and entering the gas volume of the separator typically have relatively high charge states ($q > 10$) and wide distributions [19]. This wide charge-state distribution becomes focused around the $\bar{q}$ during the movement of the ions through the first centimeters of gas behind the target before entering the dipole chamber. Consequently, the further trajectory of the ERs through the separator can be defined by applying a magnetic field which corresponds to their magnetic rigidity. The magnetic rigidity $B\rho$ of an ion moving in a magnetic field perpendicular to its velocity (υ) vector is given by the expression

$$B\rho \cong 0.0227\frac{A(\upsilon/\upsilon_0)}{\bar{q}}, \tag{1}$$

where A is the atomic mass number of the ERs. Here, $\upsilon_0 = 2.19 \times 10^8$ cm/s is the atomic unit (a.u.) of velocity. Thus, knowing the velocity and the atomic mass number of the heavy ions, their $\bar{q}$ can be directly determined by measuring $B\rho$.

The velocity of ERs is calculated in two steps. In the first step, the velocity of the ERs formed inside the solid target can be estimated from fusion-evaporation reaction kinematics. In the second step, the residual velocity of the ERs passing the distance from the target to the center of the dipole magnet (603 mm) in He gas at a given gas pressure can be estimated using the SRIM code [20]. An average uncertainty of ≈3% is estimated for the calculated velocities, which includes the uncertainties in the beam energy (0.2%) and in the thicknesses of the target backing foils (10%) and of the solid targets (10%).

In the focal plane of TASCA, a Si-strip-detector-based detection system [13,21] is installed, which is suitable for registering the implantation of the ERs and their subsequent nuclear decay. Typically, the ERs produced in fusion-evaporation reactions are unstable against β decay, α decay, and/or spontaneous fission. The atomic mass number of heavy ions can be determined through the characteristic nuclear decay modes of the ERs [22].

If the preset magnetic rigidity of the separator $(B\rho)_0$ corresponds to the $B\rho$ of the ERs, then these are centered in the focal-plane detector in a Gaussian-like distribution along the horizontal axis. As an example, we show in Fig. 1 the horizontal distributions of ^{188}Pb measured in 0.8 and 1.5 mbar He. The same TASCA magnetic setting, $(B\rho)_0 = 1.62$ Tm, was used in both measurements. For this setting and at a He pressure of $P = 0.8$ mbar, the ^{188}Pb are distributed close to the center of the focal-plane detector.

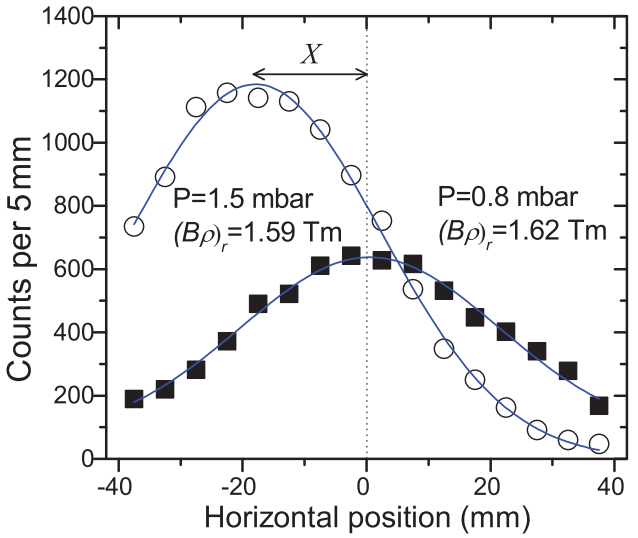

FIG. 1. (Color online) Experimental distributions of ^{188}Pb in the focal-plane detector at 0.8 (solid symbols) and 1.5 mbar (open symbols) He pressure. In both cases, TASCA was set to the same magnetic rigidity of $(B\rho)_0 = 1.62$ Tm. Lines show the fitted Gaussians. See text for details.

At 1.5 mbar pressure, the ^{188}Pb distribution in the detector is shifted, indicating that the magnetic rigidity of the ^{188}Pb ions is now different from the value preset at the separator. As described in Refs. [21,23], the real magnetic rigidity $(B\rho)_r$ corresponding to the average charge state of the detected ERs can then be estimated by the following expression:

$$(B\rho)_r = (B\rho)_0\left(1 + \frac{X}{100D}\right), \tag{2}$$

where D is the dispersion at the focal plane of TASCA in mm per 1% change in $(B\rho)_0$ [23]; in the case of TASCA, $D = 9$ mm [9]. X is the shift (in mm) of the center of the horizontal distribution relative to the center of the focal-plane detector, determined by fitting the experimental data to a Gaussian distribution. In the case of a low number of heavy ions detected at the focal-plane detector, a weighted mean value of X was taken. As an example, in the case of Fig. 1, $(B\rho)_r = 1.59$ Tm is used to deduce $\bar{q}$ at the 1.5 mbar pressure. A more detailed description of the experimental evaluation of $\bar{q}$ at gas-filled separators can be found in Refs. [21,23].

III. THEORETICAL TREATMENT OF THE DETERMINATION OF THE AVERAGE CHARGE STATES

The variation of the ions' charge-state fractions $F_q(x)$ in the gas or solid volume can be described by the balance differential equations [1],

$$\frac{dF_q(x)}{dx} = \sum_{q' \neq q}[\sigma_{q'q}F_{q'}(x) - \sigma_{qq'}F_q(x)], \tag{3}$$

$$\sum_q F_q(x) = 1, \tag{4}$$

where x is the gas or solid areal density in cm^{-2} and $\sigma_{qq'}$ and $\sigma_{q'q}$ are the charge-changing cross sections for EC and EL

processes in cm^2. At large x, the $F_q(x)$ fractions reach their equilibrium and do not change with a further increase of x, i.e., their derivatives tend to zero,

$$\frac{dF_q(x)}{dx} \to 0, \quad x \to \infty. \tag{5}$$

The average equilibrium charge state $\bar{q}$ is determined by the general relation

$$\bar{q} = \sum_q q F_q, \tag{6}$$

where F_q denote the *equilibrium* charge-state fractions. Our aim is to express the equilibrium fractions F_q through the charge-changing cross sections and, since the EL and EC processes depend on the gas density (see, e.g., [24]), to investigate the influence of the density effect on $\bar{q}$.

For He media atoms, we neglect in Eqs. (3)–(5) multiple-electron collision processes and the radiative processes, and present the equilibrium fractions F_q in terms of cross-section ratios $\sigma_{q+1,q}/\sigma_{q,q+1}$, where $\sigma_{q+1,q}$ and $\sigma_{q,q+1}$ are the *one-electron* capture and loss cross sections, respectively. In this approximation, the equilibrium charge-state fractions for ions with the charges q and $q+1$ are connected by the simple relation (see [1])

$$F_{q+1} = F_q \frac{\sigma_{q,q+1}}{\sigma_{q+1,q}}, \quad \sum_q F_q(x) = 1. \tag{7}$$

Knowing the one-electron charge-changing cross sections and using Eqs. (7) and (6), the equilibrium charge-state fractions F_q and the $\bar{q}$ are obtained.

A. Calculations of the electron orbital binding energies

The elements considered here are given in Table I together with their electronic configurations and ionization potentials (IPs). The IPs for elements with $Z \leqslant 92$ are taken from experimental works indicated in the table. For heavier elements, i.e., No to element 120, no experimental IPs are available; we thus present the best previously published theoretical values.

TABLE I. Heavy and superheavy elements considered in the present work. The electron configurations of the outer shells are given together with the ionization potentials, IP (eV).

Element	Z	Configuration	IP (eV)	Ref.
Hg	80	$5s^2\,5p^6\,5d^{10}\,6s^2$	10.438	Expt. [25]
Pb	82	$5p^6\,5d^{10}\,6s^2\,6p^2$	7.417	Expt. [26]
Fr	87	$5d^{10}\,6s^2\,6p^6\,7s^1$	4.073	Expt. [27]
Ra	88	$5d^{10}\,6s^2\,6p^6\,7s^2$	5.278	Expt. [28]
Ac	89	$6s^2 6p^6\,7s^2 6d^1$	5.380	Expt. [29]
U	92	$6p^6\,5f^3\,6d^1\,7s^2$	6.194	Expt. [30]
No	102	$6s^2\,6p^6\,5f^{14}\,7s^2$	6.632	Theor. [31]
Rf	104	$5f^{14}\,6p^6\,6d^2\,7s^2$	6.010	Theor. [32]
Fl	114	$5f^{14}\,6d^{10}\,7s^2\,7p^2$	8.538	Theor. [33]
Uup	115	$5f^{14}\,6d^{10}\,7s^2\,7p^3$	5.579	Theor. [34]
Uus	117	$5f^{14}\,6d^{10}\,7s^2\,7p^5$	7.640	Theor. [35]
Uue	119	$6d^{10}\,7s^2\,7p^6\,8s^1$	4.793	Theor. [36]
Ubn	120	$6d^{10}\,7s^2\,7p^6\,8s^2$	5.851	Theor. [37]

In general, numerical calculations of EL and EC cross sections require data on the orbital binding energies of outer as well as inner shells for both colliding particles. For the He atom, the experimental binding energy was used. Under the present experimental conditions (ion energies, He-gas pressure), it was necessary to calculate the orbital binding energies for heavy atoms and ions with the charge states $0 \leqslant q \leqslant 15$, the equilibrium fractions of which give the main contribution to the sum (6) for the $\bar{q}$. The orbital binding energies for the heavy atoms listed in Table I and their ions were calculated using two variants of the Dirac-Hartree-Fock (DHF) approach: closed-shell single-reference DHF for the closed-shell ions, and the open-shell single-determinant average-of-configuration DHF for the open-shell systems [38]. The calculations were performed within the framework of the projected Dirac-Coulomb Hamiltonian [39],

$$H_{DC} = \sum_i h_D(i) + \sum_{i<j} 1/r_{ij}. \tag{8}$$

Here, h_D is the one-electron Dirac Hamiltonian,

$$h_D(i) = c\boldsymbol{\alpha} \cdot \mathbf{p}_i + c^2\beta_i + V_{\rm nuc}(i), \tag{9}$$

where $\boldsymbol{\alpha}$ and β are the four-dimensional Dirac matrices. The nuclear potential takes into account the finite size of the nucleus, modeled by the Gaussian charge distribution [40]. Dual family basis sets of Faegri [41] were employed for all atoms, consisting of $26s24p18d13f5g2h$ orbitals. All atomic calculations were performed using the DIRAC08 computational program package [42].

B. Calculations of the charge-changing cross sections and average charge states with account for the density effect

One-electron capture and loss cross sections for heavy ions passing through a He gas were calculated using the CAPTURE and RICODE-M (Relativistic Ionization Code-Modified) computer programs described in [43] and [44], respectively.

The CAPTURE code allows calculating one-electron capture probabilities and cross sections in the normalized Brinkman-Kramers approximation. The code calculates the EC probabilities as a function of the impact parameter and the relative velocity υ, the partial cross sections $\sigma_n(\upsilon)$ for the capture into the states with the principal quantum numbers n of the scattered heavy ion, and the total (summed over all n states) capture cross sections $\sigma_{\rm tot}(\upsilon)$:

$$\sigma_{\rm tot}(\upsilon) = \sum_{n_0}^{n_{cut}} \sigma_n(\upsilon). \tag{10}$$

Here, n_0 denotes the quantum number of the ground state and n_{cut} is the maximal quantum number of the scattered heavy ion; ions created with $n > n_{cut}$ are ionized by He atoms in subsequent collisions. The n_{cut} value depends on the velocity υ, the gas density, and the atomic structure of colliding particles in accordance with the density effect: n_{cut} is large (the effect is small) for low-density volumes (a dilute gas) and fast highly charged ions, and it is small (the effect is large) for high-density volumes (a foil) and slow low-charged ions. In general, a qualitative dependence of the quantum number n_{cut}

TABLE II. The cutoff parameter n_{cut} found from Eq. (12) as a function of the He-gas pressure P for EC cross sections [Eq. (10)] of Pb^{q+} ions colliding with He atoms at 259 keV/u, $\upsilon = 3.22$ a.u.

P (mbar)	$q=1$	$q=3$	$q=5$	$q=7$	$q=9$	$q=11$
0.0	∞	∞	∞	∞	∞	∞
0.2	6	6	10	13	15	18
0.5	6	6	8	11	13	16
0.8	6	6	8	10	13	15
1.0	6	6	8	10	12	14
1.5	6	6	7	9	11	13
2.0	6	6	7	9	11	12
6.0	6	6	6	8	9	11
10.0	6	6	6	7	9	10

on the atomic parameters is given by (see [24] for details)

$$n_{cut} \approx q\left(\frac{10^{18}\ \mathrm{cm}^{-3}}{Z_a^2\rho}\right)^{1/7}\left(\frac{\upsilon^2}{10q^2}\right)^{1/14}, \qquad (11)$$

where Z_a and ρ are the nuclear charge of the gaseous or solid media atoms and the density of this volume, respectively; ρ is in cm^{-3} and velocity υ is in atomic units.

The n_{cut} was found numerically from the balance equation between ionization collision rate $\rho\upsilon\sigma_{EL}(n)$ and the total radiative decay rate $W(n)$ into lower states,

$$\rho\upsilon\sigma_{EL}(n_{cut}) = W(n_{cut}), \qquad (12)$$

where ρ is the He-gas density ($\rho \sim P$).

A typical dependence of the n_{cut} parameter on the gas pressure P and the ion charge state q in the case of Pb^{q+} ions colliding with He atoms at an energy of $E = 259$ keV/u is shown in Table II. If $P \approx 0$ (binary collisions), then the Pb ions can be created in all possible states: $n_{cut} = \infty$. As the P increases, the number n_{cut} of survived states decreases, but increases with the ion charge q. Therefore, as also seen from Table II, EC for low-charged Pb^{q+} ions with $q = 1$, 2, and 3, occurs mainly in the ground and low-excited states of the resulting ions with $q = 0$, 1, and 2.

The EL cross sections were calculated using the computer code RICODE-M described in Ref. [44]. The code is based on the relativistic Born approximation and employs relativistic values for the binding energies, the radial wave functions, and the interaction between the colliding particles, i.e., between heavy ions and He atoms.

As a typical example, Fig. 2 shows the EL cross sections for nobelium ions colliding with He atoms as a function of the ion energy calculated by the RICODE-M program. A contribution of EL from different nobelium-ion shells is shown, and it is seen that in the case of No^{2+} ions, the main contribution is given by EL from $5f$ and $6p$ shells, while for No^{8+} ions, the $5d$ electrons begin to contribute at energies higher than about 500 keV/u.

At energies higher than 1 MeV/u, it is necessary to take into account EL from many (usually 5–8) atomic shells; this requires accurate data for the binding energies of inner-shell electrons of heavy ions.

Accounting for the density effect in the calculation of the EL cross sections is a more complicated problem compared to that for EC. Roughly, the EL cross section from the ground

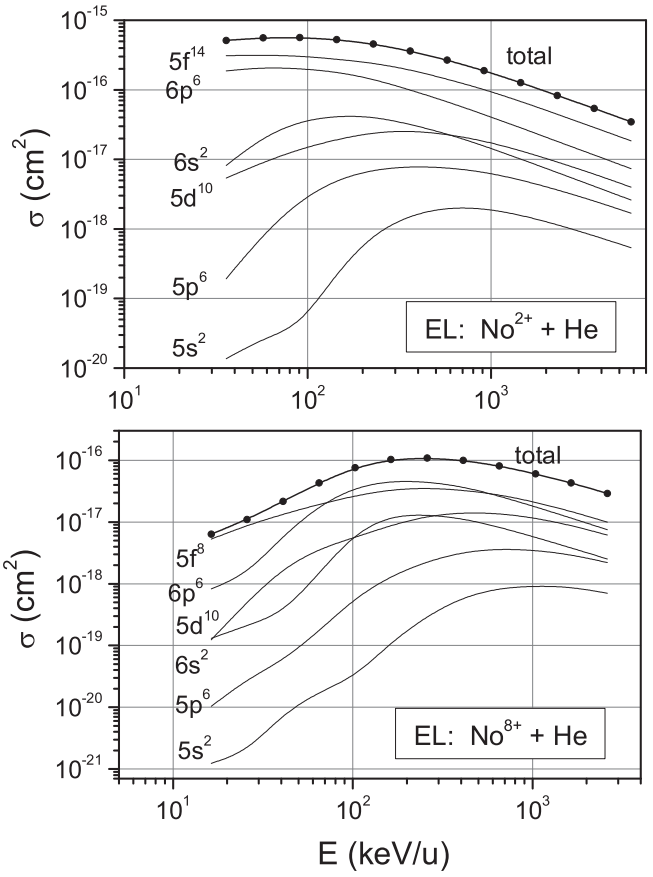

FIG. 2. Calculated EL cross sections for No^{2+} and No^{8+} ions ($Z = 102$) colliding with He atoms as a function of the ion energy. Contribution of ionization from different electron shells in No^{2+} and No^{8+} ions to the total EL cross sections is shown.

state n_0 of heavy ion accounting for the density effect can be presented as the sum [24]

$$\sigma_{\mathrm{EL}}^{DE}(n_0) \approx \sigma_{\mathrm{EL}}(n_0) + \sigma_{ex}(n_0 - n_r)\,B(n_r,\rho), \qquad (13)$$

where $B(n_r,\rho)$ is the branching ratio coefficient dependent on the gas density ρ and varying in the limits $0 < B(n_r,\rho) < 1$, and $\sigma_{\mathrm{EL}}(n_0)$ is the EL cross section where the density effect is neglected; $\sigma_{ex}(n_0 - n_r)$ is the excitation cross section for the resonant (electric-dipole-allowed) transition $n_0 \longrightarrow n_r$, where n_r is the principal quantum number of the resonance level. For all of the ions and the He-gas pressures considered in this work, the calculated excitation cross sections are much smaller compared to the EL ones, i.e.,

$$\sigma_{ex}(n_0 - n_r) \ll \sigma_{\mathrm{EL}}(n_0). \qquad (14)$$

Therefore, the influence of the density effects on the EL cross sections for a fixed ion charge state q was found to be negligible, i.e., the EL cross sections remain approximately independent of the gas pressure. Such a behavior of the EL cross sections has been experimentally found in Ref. [45], where the influence of the density effect on EC cross sections is much stronger than on EL ones within the gas-pressure range close to the pressures used here.

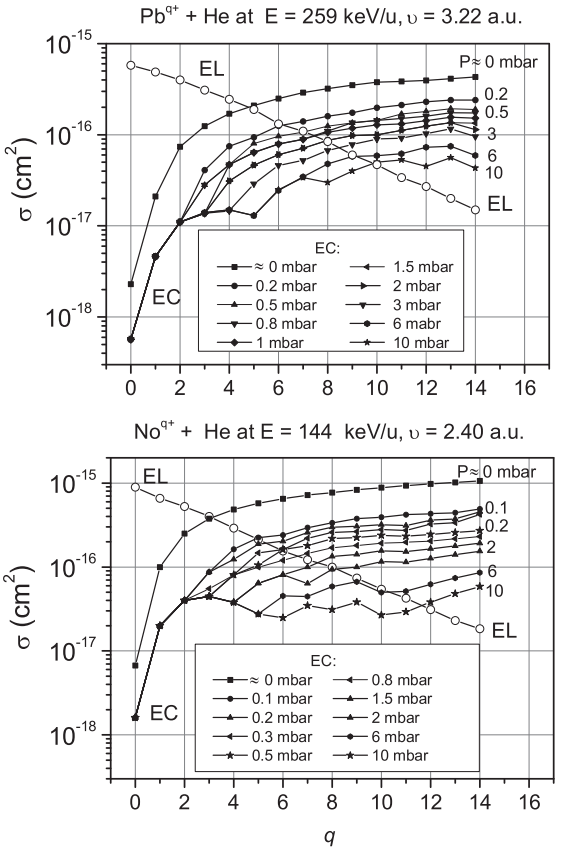

FIG. 3. Calculated charge-changing cross sections for Pb^{q+} ($Z = 82$) and No^{q+} ($Z = 102$) ions colliding with He atoms as a function of the ion charge q at different gas pressures $P \approx 0$–10 mbar (see also Table II). Solid curve with open circles: EL cross section, the RICODE-M program; solid curves with solid symbols: EC cross sections at different gas pressures, the CAPTURE code.

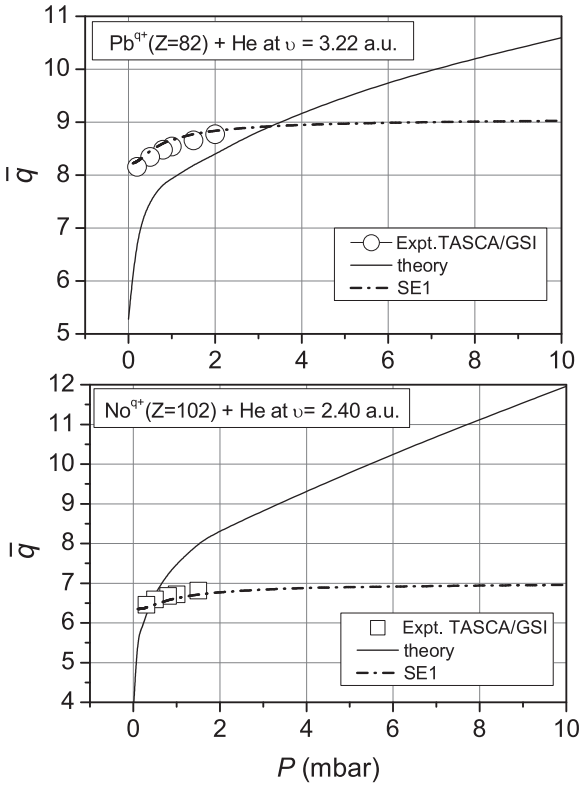

FIG. 4. Average charge states as a function of the gas pressure P for Pb^{q+} and No^{q+} ions colliding with He atoms. Experimental data [21] are shown by the open symbols. The error bars are smaller than the size of the symbols. Solid and dash-dotted lines mark the results of the present theoretical calculations and of the semiempirical approach SE1, respectively (see text).

IV. RESULTS OF THE CALCULATIONS AND COMPARISON WITH EXPERIMENT; THE INFLUENCE OF THE DENSITY EFFECT

Calculated charge-changing cross sections for Pb and No ions colliding with He atoms are shown in Fig. 3 as a function of the ion charge states and He-gas pressure. As was mentioned before, EL cross sections are independent of the gas pressure, while the EC cross sections exhibit a strong dependence on P due to the influence of the density effect. We note that in the figure, the q values correspond to the initial state for the EL cross sections and to the final state for the EC cross sections in accordance with Eq. (7). For example, at $q = 0$, the EL cross section corresponds to the ionization of a neutral atom into a singly charged ion, and the EC cross section corresponds to the creation of a neutral atom from a singly charged ion. EL curves cross a series of EC cross-section curves at points roughly corresponding to the $\bar{q}$ at a given pressure. The $\bar{q}$ values estimated from Fig. 3 increase from 5 to 10 for Pb ions and from 3 to 12 for No ions with increasing pressure from 0 to 10 mbar. Obviously, the density effect is large.

The experimental and the calculated $\bar{q}$ values for Pb and No ions are presented in Fig. 4 as a function of the He-gas pressure. Experimental $\bar{q}$ values of both ions are smoothly increasing with increasing gas pressure, indicating the presence of the density effect. In the case of Pb ions, the smooth dependence is fairly well reproduced by theory, while for the No ions, the calculations show a much stronger dependence on the gas pressure than the experimental data. This discrepancy may be attributed to assumptions made in the present theoretical framework. One is related to the choice of the n_{cut} parameter for EC cross sections which is not unique. There are a few formulas for n_{cut} (see, e.g., [24]); we used Eq. (12), which provides the best agreement with experiment at 0.8 mbar pressure. Another reason may be related to the fact that we neglected multielectron processes in the calculations. At velocities $\upsilon \approx 1$–4 a.u. as considered here, double-electron loss and double-electron capture processes can provide a considerable contribution. The influence of the specific selection of the n_{cut} parameter and of multielectron processes on the theoretical $\bar{q}$ values will be further investigated in the future.

In Fig. 4, the results of a semiempirical approach (hereafter, SE1) are also shown by the dash-dotted curves. These $\bar{q}_{\rm SE1}$ values were obtained in two steps. Initially, a semiempirical formula given in Ref. [46] was used to obtain the $\bar{q}$ values. However, these $\bar{q}$ values are only valid for a fixed He-gas pressure of 0.66 mbar. Therefore, in order to incorporate the gas-pressure influence into these results, the density-effect correction as suggested in Ref. [21] was applied.

The results for the experimental $\bar{q}_{\rm exp}$ and the calculated $\bar{q}_{th}$ average charge states for elements considered here are

TABLE III. Experimental ($\bar{q}_{\rm exp}$) and calculated $\bar{q}$ of heavy and superheavy ions. The identified evaporation residue (ER), atomic numbers (Z), nuclear reactions, ion velocities, and the measured He-gas pressures are also given. The results of Bohr's predictions $\bar{q}_B$ [47] and two different semiempirical approaches, $\bar{q}_{\rm SE1}$ (see text) and $\bar{q}_{\rm SE2}$ [48], are presented together with theoretical $\bar{q}_{th}$ results obtained in this work.

ER	Z	Reaction	v (a.u.)	P (mbar)	$\bar{q}_{\rm exp}$	$\bar{q}_B$	$\bar{q}_{\rm SE1}$	$\bar{q}_{\rm SE2}$	$\bar{q}_{th}$
^{180}Hg	80	^{144}Sm(^{40}Ar,4n)	2.84	0.6	6.97 ± 0.30	12.2	7.40	9.07	6.04
^{188}Pb	82	^{144}Sm(^{48}Ca,4n)	3.22	0.8	8.45 ± 0.19	14.0	8.60	10.55	7.83
^{205,206}Fr	87	^{181}Ta(^{30}Si,3-4n)	2.04	0.5	5.67 ± 0.19	9.0	6.06	6.46	5.96
$^{209-211}$Ra	88	^{158,160}Gd(^{54}Cr,3-4n)	3.17	0.6	9.37 ± 0.31	14.1	9.22	10.47	8.05
^{215}Ac	89	^{179}Au(^{22}Ne,4n)	1.39	0.8	4.28 ± 0.42	6.2	4.20	4.22	5.75
^{221,222}U	92	^{176}Yb(^{50}Ti,4-5n)	2.89	0.8	8.76 ± 0.29	13.0	8.64	9.80	8.27
^{252,254}No	102	^{206,208}Pb(^{48}Ca,2n)	2.40	0.8	6.68 ± 0.18	11.2	6.57	8.30	7.23
$^{254-256}$Rf	104	^{206,208}Pb(^{50}Ti,1-2n)	2.65	0.8	7.32 ± 0.25	12.5	7.30	9.37	7.02
^{288}Fl	114	^{244}Pu(^{48}Ca,4n)	2.30	0.8	6.70 ± 0.37	11.1	6.97	8.28	8.02
^{287,288}Uup	115	^{243}Am(^{48}Ca,3-4n)	2.28	0.8		11.1	7.03	8.23	7.70
^{293,294}Uus	117	^{249}Bk(^{48}Ca,3-4n)	2.25	0.8		11.0	7.16	8.19	8.58
^{295,296}Uue	119	^{249}Bk(^{50}Ti,3-4n)	2.42	0.8		11.9	7.83	8.92	8.73
^{295,296}Ubn	120	^{249}Cf(^{50}Ti,3-4n)	2.43	0.8		12.0	7.93	9.02	9.03

summarized in Table III, where the ERs from the corresponding fusion-evaporation reactions, atomic numbers of the elements, ion velocities, and the He-gas pressures are also given. The velocities and gas pressures used in the calculation of the $\bar{q}_{th}$ for $Z = 115, 117, 119$, and 120 were those as applied in the corresponding experiments at TASCA [16,18]. The $\bar{q}_{th}$ values agree with $\bar{q}_{\rm exp}$ within 20%, except for the Ac ions where the deviation is 34%. In this case, the measurement was performed at a rather low velocity of 1.49 a.u. This may indicate that at such low velocities, the computer codes used here no longer provide reliable results.

A well-known dependence of the $\bar{q}$ on the ion's atomic number Z and velocity v was obtained in Bohr's semiclassical model [47],

$$\bar{q}_B = (v/v_0)Z^{1/3}, \tag{15}$$

for a velocity range $1 < (v/v_0) < Z^{2/3}$. In this model, $\bar{q}$ does not depend on the initial charge-state distribution of the incident ions, the atomic number of the gas-target atom, or the gas pressure.

The estimated $\bar{q}_B$ and the results from the two semiempirical approaches $\bar{q}_{\rm SE1}$ and $\bar{q}_{\rm SE2}$ [48] are also presented in Table III. The results obtained using Bohr's formula significantly overestimate the experimental data, probably because this formula neglects the dependencies on the target atomic number and the gas pressure.

Another type of semiempirical formula $\bar{q}_{\rm SE2}$ was obtained in Ref. [48] on the basis of experimental charge-state distributions of various ions with $Z = 1$–92 passing through gaseous media with $Z_a = 1$–54. This formula was obtained as a least-squares fit of experimental data given in Ref. [1] and takes into account the dependence on the nuclear charge of the gas atoms, but not on the gas pressure. As is seen from Table III, $\bar{q}_{\rm SE2}$ are in poorer agreement with the experiment than $\bar{q}_{\rm SE1}$ (see below). This is in line with the expectation that the semiempirical formula derived from fits to experimental data perform best for the prediction of data in similar experimental conditions.

The $\bar{q}_{\rm SE1}$ agrees well (within 7%) with the present experimental data. In the region of the heavy elements $Z = 102$ and 104, the agreement of the $q_{\rm SE1}$ data with the experiment is particularly good (within ≈2%).

The semiempirical formula [46] used in the SE1 approach contains two terms, which are parameterized by a fit to experimental data up to Rg ($Z = 111$) obtained at a pressure of 0.66 mbar [46]. The first term is given as a modified version of Bohr's formula. The second term takes into account the atomic shell structure of the stripped ions. This formula underestimates the experimental $\bar{q}$ of Fl ($Z = 114$) by about 5% [10–13] (see also Table III), which can drastically affect the success of the long-term superheavy-element research campaigns, where only few ions are expected to be produced [3,18,49]. Presently, the SE1 approach with a slight modification of the shell correction term in the semiempirical formula of Ref. [46] is used in the planning of the experiments at TASCA [50]. The estimated $\bar{q}$ values for the elements with $Z = 114$, 115, 117, 119, and 120 are 6.65, 6.73, 6.79, 7.52, and 7.59, respectively [50]. The experimental mean value of $\bar{q}$(Fl) = 6.70 (see Table III) is predicted to within 1%. The recent experiments on the production of these superheavy elements at TASCA were based on the magnetic rigidities corresponding closely to these predicted $\bar{q}$ values [16–18].

V. SUMMARY AND CONCLUSION

Experimental data for the average charge states $\bar{q}$ for heavy and superheavy ions with atomic numbers $80 \leqslant Z \leqslant 114$ passing through dilute He gas are presented. The energy of the ions was a few hundred keV/u and the He-gas pressure was about 0.8 mbar. The measured $\bar{q}$ values are in the range $4 < \bar{q} < 10$. Experimental data were compared with predictions of several semiempirical approaches.

Calculations of the $\bar{q}$ values were performed on the basis of atomic calculations of one-electron capture and loss cross sections, taking into account the atomic structure of heavy ions and the density effect of the He gas. The calculated $\bar{q}$ values agree with experimental data within 20%. On the basis of the present atomic calculations, the $\bar{q}$ of superheavy elements with atomic numbers $Z = 115$, 117,

119, and 120 were predicted. The dependence of the average charge state on the He-gas pressure was taken into account in the calculations, and found to be important. In order to obtain better agreement with the experimental $\bar{q}$ values, further investigations accounting for multielectron collision loss and capture cross sections are necessary.

ACKNOWLEDGMENTS

The authors are grateful to the HIM Fellow research program for financial support provided to one of us (V.P.S) and to Dr. V. Pershina for initiating this fruitful collaboration. This work was also partly supported by Grant No. 11-02-00526-a of the Russian Foundation for Basic Research.

[1] H.-D. Betz, Rev. Mod. Phys. **44**, 465 (1972).
[2] S. Hofmann and G. Münzenberg, Rev. Mod. Phys. **72**, 733 (2000).
[3] Yu. Ts. Oganessian, J. Phys. G **34**, R165 (2007).
[4] Yu. Oganessian, Radiochim. Acta **99**, 429 (2011).
[5] A. Ghiorso, S. Yashita, M. E. Leino, L. Frank, J. Kalnins, P. Armbruster, J.-P. Dufour, and P. K. Lemmertz, Nucl. Instrum. Methods A **269**, 192 (1988).
[6] K. Morita, A. Yoshida, T. T. Inamura, M. Koizumi, T. Nomura, M. Fujioka, T. Shinozuka, H. Miyatake, K. Sueki, H. Kudo, Y. Nagai, T. Toriyama, K. Yoshimura, and Y. Hatsukawa, Nucl. Instrum. Methods B **70**, 220 (1992).
[7] M. Leino, Nucl. Instrum. Methods B **126**, 320 (1997).
[8] K. Subotic, Yu. Ts. Oganessian, V. K. Utyonkov, Yu.V. Lobanov, F. Sh. Abdullin, A. N. Polyakov, Yu. S. Tsyganov, and O. V. Ivanov, Nucl. Instrum. Methods A **481**, 71 (2002).
[9] A. Semchenkov, W. Brüchle, E. Jäger, E. Schimpf, M. Schädel, C. Mühle, F. Klos, A. Türler, A. Yakushev, A. Belov, T. Belyakova, M. Kaparkova, V. Kukhtin, E. Lamzin, and S. Sytchevsky, Nucl. Instrum. Methods B **266**, 4153 (2008).
[10] L. Stavsetra, K. E. Gregorich, J. Dvorak, P. A. Ellison, I. Dragojevic, M. A. Garcia, and H. Nitsche, Phys. Rev. Lett. **103**, 132502 (2009).
[11] P. A. Ellison, K. E. Gregorich, J. S. Berryman, D. L. Bleuel, R. M. Clark, I. Dragojevic, J. Dvorak, P. Fallon, C. Fineman-Sotomayor, J. M. Gates, O. R. Gothe, I. Y. Lee, W. D. Loveland, J. P. McLaughlin, S. Paschalis, M. Petri, J. Qian, L. Stavsetra, M. Wiedeking, and H. Nitsche, Phys. Rev. Lett. **105**, 182701 (2010).
[12] Ch. E. Düllmann, M. Schädel, A. Yakushev, A. Türler, K. Eberhardt, J. V. Kratz, D. Ackermann, L.-L. Andersson, M. Block, W. Brüchle, J. Dvorak, H. G. Essel, P. A. Ellison, J. Even, J. M. Gates, A. Gorshkov, R. Graeger, K. E. Gregorich, W. Hartmann, R.-D. Herzberg, F. P. Heßberger, D. Hild, A. Hübner, E. Jäger, J. Khuyagbaatar, B. Kindler, J. Krier, N. Kurz, S. Lahiri, D. Liebe, B. Lommel, M. Maiti, H. Nitsche, J. P. Omtvedt, E. Parr, D. Rudolph, J. Runke, B. Schausten, E. Schimpf, A. Semchenkov, J. Steiner, P. Thörle-Pospiech, J. Uusitalo, M. Wegrzecki, and N. Wiehl, Phys. Rev. Lett. **104**, 252701 (2010).
[13] J. M. Gates, Ch. E. Düllmann, M. Schädel, A. Yakushev, A. Türler, K. Eberhardt, J. V. Kratz, D. Ackermann, L.-L. Andersson, M. Block, W. Brüchle, J. Dvorak, H. G. Essel, P. A. Ellison, J. Even, U. Forsberg, J. Gellanki, A. Gorshkov, R. Graeger, K. E. Gregorich, W. Hartmann, R.-D. Herzberg, F. P. Heßberger, D. Hild, A. Hübner, E. Jäger, J. Khuyagbaatar, B. Kindler, J. Krier, N. Kurz, S. Lahiri, D. Liebe, B. Lommel, M. Maiti, H. Nitsche, J. P. Omtvedt, E. Parr, D. Rudolph, J. Runke, H. Schaffner, B. Schausten, E. Schimpf, A. Semchenkov, J. Steiner, P. Thörle-Pospiech, J. Uusitalo, M. Wegrzecki, and N. Wiehl, Phys. Rev. C **83**, 054618 (2011).
[14] R. C. Barber, P. J. Karol, H. Nakahara, E. Vardaci, and E. W. Vogt, Pure Appl. Chem. **83**, 1485 (2011).
[15] R. D. Loss and J. Corish, Pure Appl. Chem. **84**, 1669 (2012).
[16] D. Rudolph *et al*., Phys. Rev. Lett. **111**, 112502 (2013).
[17] Ch. E. Düllmann, A. Yakushev, J. Khuyagbaatar, D. Rudolph, H. Nitsche *et al*., GSI Scientific, Report No. 2012-1, 206, 2012; http://www.gsi.de/library/GSI-Report-2012-1/.
[18] J. Khuyagbaatar, A. Yakushev, Ch. E. Düllmann, H. Nitsche, J. Roberto *et al*., GSI Scientific, Report No. 2013-1, 131, 2012; http://www.gsi.de/library/GSI-Report-2013-1/.
[19] V. S. Nikolaev and I. S. Dmitriev, Phys. Lett. A **28**, 277 (1968).
[20] J. F. Ziegler, Nucl. Instrum. Methods B **219**, 1027 (2004).
[21] J. Khuyagbaatar, D. Ackermann, L.-L. Andersson, J. Ballof, W. Brüchle, Ch. E. Düllmann, J. Dvorak, K. Eberhardt, J. Even, A. Gorshkov, R. Graeger, F.-P. Heßberger, D. Hild, R. Hoischen, E. Jäger, B. Kindler, J. V. Kratz, S. Lahiri, B. Lommel, M. Maiti, E. Merchan, D. Rudolph, M. Schädel, H. Schaffner, B. Schausten, E. Schimpf, A. Semchenkov, A. Serov, A. Türler, and A. Yakushev, Nucl. Instrum. Methods A **689**, 40 (2012).
[22] R. B. Firestone, V. S. Shirley, C. M. Baglin, S. Y. Frank Chu, and J. Zipkin, *Table of Isotopes*, 8th ed. (Wiley, New York, 1996).
[23] Yu. Ts. Oganessian, V. K. Utyonkov, Yu. V. Lobanov, F. Sh. Abdullin, A. N. Polyakov, I. V. Shirokovsky, Yu. S. Tsyganov, A. N. Mezentsev, S. Iliev, V. G. Subbotin, A. M. Sukhov, G. V. Buklanov, K. Subotic, Yu. A. Lazarev, K. J. Moody, J. F. Wild, N. J. Stoyer, M. A. Stoyer, R. W. Lougheed, and C. A. Laue, Phys. Rev. C **64**, 064309 (2001).
[24] V. P. Shevelko, H. Tawara, O. V. Ivanov, T. Miyoshi, K. Noda, Y. Sato, A. V. Subbotin, and I. Yu. Tolstikhina, J. Phys. B **38**, 2675 (2005).
[25] M. A. Baig, J. Phys. B **16**, 1511 (1983).
[26] D. R. Wood and K. L. Andrew, J. Opt. Soc. Am. **58**, 818 (1968).
[27] E. Arnold, W. Borchers, H. T. Duong, P. Juncar, J. Lerme, P. Lievens, W. Neu, R. Neugart, M. Pellarin, J. Pinard, J. L. Vialle, K. Wendt, and ISOLDE, J. Phys. B **23**, 3511 (1990).
[28] J. A. Armstrong, J. J. Wynne, and F. S. Tomkins, J. Phys. B **13**, L133 (1980).
[29] J. Roßnagel, S. Raeder, A. Hakimi, R. Ferrer, N. Trautmann, and K. Wendt, Phys. Rev. A **85**, 012525 (2012).
[30] A. Coste, R. Avril, P. Blancard, J. Chatelet, D. Lambert, J. Legre, S. Liberman, and J. Pinard, J. Opt. Soc. Am. **72**, 103 (1982).
[31] A. Borschevsky, E. Eliav, M. J. Vilkas, Y. Ishikawa, and U. Kaldor, Phys. Rev. A **75**, 042514 (2007).
[32] E. Eliav, U. Kaldor, and Y. Ishikawa, Phys. Rev. Lett. **74**, 1079 (1995).

[33] A. Landau, E. Eliav, Y. Ishikawa, and U. Kaldor, J. Chem. Phys. **114**, 2977 (2001).
[34] E. Eliav, U. Kaldor, and Y. Ishikawa, Mol. Phys. **94**, 181 (1998).
[35] Zh. Chang, J. Li, and Ch. Dong, J. Phys. Chem. A **114**, 13388 (2010).
[36] E. Eliav, M. J. Vilkas, Y. Ishikawa, and U. Kaldor, Chem. Phys. **311**, 163 (2005).
[37] A. Borschevsky, V. Pershina, E. Eliav, and U. Kaldor, Phys. Rev. A **87**, 022502 (2013).
[38] J. Thyssen, Ph.D. thesis, University of Southern Denmark, 2001.
[39] J. Sucher, Phys. Rev. A **22**, 348 (1980).
[40] L. Visscher and K. G. Dyall, At. Data Nucl. Data Tables **67**, 207 (1997).
[41] K. Faegri, Theor. Chim. Acta **105**, 252 (2001).
[42] L. Visscher, H. J. Aa. Jensen, T. Saue, R. Bast, S. Dubillard, K. G. Dyall, U. Ekström, E. Eliav, T. Fleig, A. S. P. Gomes, T. U. Helgaker, J. Henriksson, M. Iliaš, Ch. R. Jacob, S. Knecht, P. Norman, J. Olsen, M. Pernpointner, K. Ruud, P. Sałek, and J. Sikkema, computer code DIRAC, release DIRAC08 (2008). DIRAC is a relativistic *ab initio* electronic structure program; see http://dirac.chem.vu.nl.
[43] V. P. Shevelko, O. Rosmej, H. Tawara, and I. Yu. Tolstikhina, J. Phys. B **37**, 201 (2004).
[44] I. Yu. Tolstikhina, I. I. Tupitsyn, S. N. Andreev, and V. P. Shevelko (unpublished).
[45] G. Ryding, H. D. Betz, and A. Wittkower, Phys. Rev. Lett. **24**, 123 (1970).
[46] K. E. Gregorich, W. Loveland, D. Peterson, P. M. Zielinski, S. L. Nelson, Y. H. Chung, Ch. E. Düllmann, C. M. Folden, K. Aleklett, R. Eichler, D. C. Hoffman, J. P. Omtvedt, G. K. Pang, J. M. Schwantes, S. Soverna, P. Sprunger, R. Sudowe, R. E. Wilson, and H. Nitsche, Phys. Rev. C **72**, 014605 (2005).
[47] N. Bohr, Phys. Rev. **58**, 654 (1940).
[48] G. Schiwietz and P. L. Grande, Nucl. Instrum. Methods B **175**, 125 (2001).
[49] K. Morita, K. Morimoto, D. Kaji, H. Haba, K. Ozeki, Y. Kudou, T. Sumita, Y. Wakabayashi, A. Yoneda, K. Tanaka, S. Yamaki, R. Sakai, T. Akiyama, S. Goto, H. Hasebe, M. Huang, T. Huang, E. Ideguchi, Y. Kasamatsu, K. Katori, Y. Kariya, H. Kikunaga, H. Koura, H. Kudo, A. Mashiko, K. Mayama, S. Mitsuoka, T. Moriya, M. Murakami, H. Murayama, S. Namai, A. Ozawa, N. Sato, K. Sueki, M. Takeyama, F. Tokanai, T. Yamaguchi, and A. Yoshida, J. Phys. Soc. Jpn. **81**, 103201 (2012).
[50] J. Khuyagbaatar (unpublished).